Proceedings of the Combustion Institute 41 (2025) 105932

Contents lists available at ScienceDirect

Proceedings of the Combustion Institute

journal homepage: www.elsevier.com/locate/proci

Investigation of hot-spot-induced pre-ignition in methanol- and hydrogen-fueled spark-ignition engines

D. Golc [a,*], S. Esposito [b], M. Khosravi [c], J. Beeckmann [a], H. Pitsch [a]

[a] Institute for Combustion Technology (ITV), RWTH Aachen University, 52056 Aachen, Germany
[b] IAAPS, Department of Mechanical Engineering, University of Bath, BA2 7AY Bath, United Kingdom
[c] FORD Werke GmbH, 50735 Cologne, Germany

ARTICLE INFO

Keywords:
Hydrogen
Methanol
Hot-spot-induced pre-ignition
Internal combustion engine

ABSTRACT

The transition of the transport sector towards more sustainable propulsion requires the adoption of alternative fuels. Methanol and hydrogen are promising options because of their possible renewable production pathways, low to zero carbon content, low pollutant emission, and potential for reaching higher thermal efficiencies. A drawback is that hydrogen and methanol are more prone to hot-spot-induced pre-ignition (PI) due to their lower minimum ignition energy compared to conventional fuels. Hot-spot-induced PI can occur in engines due to hot surfaces acting as ignition points, which is a limiting factor for operation, safety and efficiency. Although undesirable in spark ignition engines (SI), hot-spot-induced ignition can facilitate the use of low-cetane fuels such as methanol and hydrogen in compression ignition engines (CI). Understanding the effects leading to hot-spot-induced pre-ignition is essential for both suppressing the phenomenon in SI engines and leveraging it in CI engines. This study investigates hot-spot-induced PI phenomena using an SI single-cylinder research engine featuring a prototype glow-plug equipped with an integrated thermocouple in order to create a controlled hot spot inside the combustion chamber. Methanol has been introduced in the combustion chamber with a direct injection (DI), while hydrogen with a port fuel injector (PFI). A parametric study was conducted using methanol and hydrogen to identify dependencies of PI events linked to certain engine operating parameters. A comprehensive data analysis featuring 3D Reynolds averaged Navier Stokes (RANS) and chemical kinetics simulations were conducted to explain the main mechanisms responsible for PI. Generally, hydrogen requires a higher hot-spot temperature to achieve pre-ignition compared to methanol. For methanol, this study provides insights into the dependencies of various parameters on the ignition timing in CI applications, allowing potentially to achieve a controllable CI combustion with glow-plug assistance. An important finding is that while methanol combustion can be effectively controlled through glow-plug temperature, the study demonstrates that such controllability is more challenging for hydrogen. Indeed, numerous parameters influencing hot-spot-induced ignition were identified. In particular, the local mixture composition near the glow-plug and elevated pressures were found to significantly impact the onset of PI, with higher pressures effectively suppressing pre-ignition. This counterintuitive behavior is explained by the inverse pressure dependence of ignition delay times for hydrogen and analyzed with reaction pathway analysis. Overall, it was observed that by adjusting the operating parameters, the potential hot-spot temperature required to trigger PI could be optimized, allowing for an increase of up to 100 K. These insights are essential for developing strategies to control or prevent PI in order to enable a safer and more efficient use of methanol and hydrogen in future engines. This experimental study provides a solid dataset for future work and validation of numerical models.

1. Introduction

Hydrogen and methanol are being extensively investigated as potential alternative fuels to power hard-to-electrify sectors such as heavy-duty, marine, and off-road [1]. Both have favorable combustion and emission characteristics and can be produced in renewable ways with simpler processes than more complex e-fuels [2,3]. Abnormal combustion like hot-spot-induced pre-ignition (PI) has been investigated mainly as a harmful phenomenon for combustion systems, especially in the context of spark-ignition (SI) internal combustion engines [4]

* Corresponding author.
E-mail address: d.golc@itv.rwth-aachen.de (D. Golc).

https://doi.org/10.1016/j.proci.2025.105932
Received 2 May 2025; Accepted 2 September 2025
Available online 1 November 2025
1540-7489/© 2025 The Authors. Published by Elsevier Inc. on behalf of The Combustion Institute. This is an open access article under the CC BY license (http://creativecommons.org/licenses/by/4.0/).

or flashback in burners [5]. However, because of future development of combustion systems with alternative fuels, a fundamental understanding of hot-spot-induced ignition properties of fuels like methanol and hydrogen can be crucial for suppressing the phenomenon in SI engines and also for gas turbines or industrial burners. Moreover, this understanding can potentially be leveraged to retrofit compression ignition (CI) engines with those fuels [6,6–12] or for alternative low-temperature combustion concepts [13].

Methanol pre-ignition has been observed both as a sporadic phenomenon triggered by various sources as well as a sustained phenomenon triggered at high loads and speed because of hot spots in the combustion chamber [14]. However, due to the relatively high knock resistance of methanol for SI engine application, the systematic study of hot-spot-induced PI has been historically more motivated by the intention to trigger methanol auto-ignition in compression ignition engines by a glow-plug in both experimental work [8–11,15] from the 90s and early 2000s and more recent computational studies [6,12]. The majority of the experimental studies [8–10] demonstrated feasibility and performance of methanol-fueled CI engines. One study from Mueller and Musculus [11] featured optical measurements that provided more insights on the hot-spot-induced phenomenology and validation data recently used in computational studies for validation [12]. To the authors' knowledge, no experimental study has featured hot-spot temperature measurement.

Regarding hydrogen, more extensive studies into PI, knock, backfiring, and generally auto-ignition can be found in the literature. The critical nature of those phenomena affects the safety, efficiency, and operability of hydrogen combustion systems [16,17]. Fundamental studies featuring simulations [18–23] or experimentally investigated combustion vessels [24] focused on highlighting the underlying basic dependencies of hydrogen hot-spot-induced ignition with air–fuel ratio, pressure, temperature, and catalytic properties of the surface. These studies concluded that the most relevant parameters for hot-spot-induced ignition are the temperature of the glow-plug followed by the initial pressure of the mixture and the equivalence ratio. The temperature of the mixture and the hot-spot area have less influence. The key parameters in preventing the PI event are reducing the gas temperature before the spark timing and the hot spot temperatures for the hydrogen case, which are parameters that are usually difficult to reduce as these values are dependent on engine load and speed conditions [4,25–28]. Recently, Rajasegar et al. [4] presented an experimental study on a heavy-duty optical engine fueled with hydrogen and operated with a glow-plug. They observed a strong dependency of PI with mixture homogenization and the start of injection. For a deeper understanding, Chu et al. performed a DNS study showing that surface ignition is fundamentally set by a critical hot-spot size and radical diffusion, with catalytic effects markedly prolonging ignition delays [23]. However, information on hot-spot temperature was lacking for detailed analysis and future validation of computational studies.

This study investigates hot-spot-induced pre-ignition (PI) initiated by an artificial hot-spot, which was generated using a prototype glow-plug under engine-relevant conditions. Primary objectives are to highlight the differences in hot-spot-induced ignition behavior between methanol and hydrogen and to identify key parameters influencing ignition for developing glow-plug-assisted combustion concepts. Moreover, also because of the determination of the glow-plug temperature, this study provides valuable datasets of hot-spot-induced conditions for further validation of computational studies.

2. Experimental setup

The engine utilized in this study is a single-cylinder DI spark-ignition (SI) research engine operated at the Institute for Combustion Technology (ITV) of RWTH Aachen University. It has four valves, high-tumble intake ports, a pent-roof combustion chamber, and a centrally positioned spark-plug and injector.

Table 1
Single-cylinder engine data for this work. Entries marked with * refer to 1 mm lift.

Parameter	Value
Displacement/cm^3	333
Bore & stroke/mm	71.9 & 82
Compression ratio/–	11.4:1
Inj. pressure DI & PFI/MPa	20 & 0.6
Int.& exh. event * /CA	184/185°
Exh. valve closing * /CAaTDC	360°

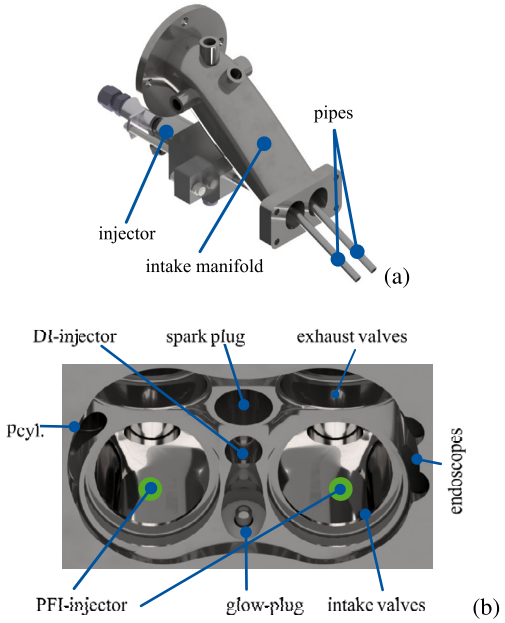


Fig. 1. a: Intake runner with the designed two pipes for PFI directed toward the intake valves. b: Cylinder-head geometry showing the positions of all sensors and devices.

The engine is coupled to a dynamometer to regulate engine speed within $\pm 2\,\mathrm{min}^{-1}$. A conditioning unit maintains the engine oil and coolant temperature at 90 °C. Instantaneous pressure measurements in the intake and exhaust ports are recorded using Kistler 4049B piezoresistive transducers, while type-K thermocouples capture average temperature readings. Cylinder pressure is monitored with a Kistler 6041 A cooled piezoelectric sensor. Crank angle (CA) resolved measurements have been recorded with an indication system by IAV GmbH at a frequency of 0.1 °CA.

To ensure repeatability, reference engine load points are recorded at each start-up throughout the measurement campaign. The key engine specifications considered in this study are summarized in Table 1. This setup has been previously used in various studies featuring gasoline and methanol for combustion and pollutant modeling [29–33].

To enable hydrogen operation, the engine was equipped with a hydrogen port fuel injection (PFI) system in the intake runner. To allow to get the hydrogen as close as possible to the intake valves, two small pipes with a length of 150 mm and 4 mm internal diameter have been added to the PFI injector, as shown in Fig. 1a. The volume of the pipes is 188.5 mm^3, which corresponds to approximately 8%–14% of the injected hydrogen remaining in those injection pipes. Because of the pipes' dimension and the stagnant flow in the pipes without injection, it can be assumed that the hydrogen release from the pipes after injection is minor and negligible. The addition of the pipes significantly reduced the occurrence of backfiring, which was previously observed due to residual mixtures of the previous cycle in the intake ports.

For scientific research on hot-spot-induced pre-ignition (PI), the engine was equipped with a controllable glow-plug featuring a Type-K

Table 2
Measurement operating conditions summarizing all varied parameters for hydrogen and methanol. [air–fuel-ratio (λ), start of energizing (SOE), intake valve closing (IVC), end compression pressure (ECP), and engine speed (n_{eng})].

Parameter	Methanol - DI (CH_3OH)	Hydrogen - PFI (H_2)
λ/–	**1.0** ‖ 1.2 ‖ 1.4 ‖ 1.6	**2.0** ‖ 3.0 ‖ 4.0
ECP/bar	20 ‖ **25** ‖ 30	25 ‖ **30** ‖ 35
SOE/°CAaTDC	−240 ‖ **−260** (H_2) ‖ **−280** (CH_3OH) ‖−300 ‖ −320	
IVC/°CAaTDC	−160 ‖ **−180** ‖ −193	
n_{eng}/rpm	1000 ‖ 1500 ‖ **2000** ‖ 2500	

thermocouple in the glow-plug tip. Similar setups have already been used to investigate hot-spot-induced characteristics with alternative fuels [34] by triggering pre-ignition at controlled and safe conditions. Fig. 1b illustrates the cylinder-head design, showing the centrally located DI injector, the locations of the two pipes connected to the PFI injector, the cylinder-head sensor (p_{cyl}), and the spark-plug. The glow-plug is installed with a custom-designed adapter in an available bore between the two intake ports. The distance between the electrode of the spark-plug and the glow-plug is 28 mm. The additional endoscope bores on the side between intake and exhaust valves can enable optical investigations (not used in this study).

3. Methodology

3.1. Experimental

To investigate the hot-spot-induced ignition tendency of methanol and hydrogen, the key parameters of interest include pressure, temperature, and air–fuel ratio, as these directly influence the ignition delay time of the mixture. The start of energizing (SOE) of the injector is also considered as a parameter affecting mixture distribution within the combustion chamber and around the glow-plug. The intake valve closing (IVC) is examined, as it can influence the inflow conditions and the mixture formation, particularly for PFI operation. Different load/pressure conditions have been reproduced by starting from a very retarded SI combustion (with glow-plug off) that reached a selected end-compression pressure (ECP). The ECP was adjusted with the boost pressure so that the gas mixture with fuel reaches the desired ECP at TDC, with the start of combustion occurring well after TDC. Table 2 summarizes the parameters investigated for both fuels. For each glow-plug temperature, 1000 consecutive cycles were recorded to establish a significant database for statistical analysis. This value was chosen as a trade-off between having sufficient data for the analysis and considering the stress on the engine parts due to pre-ignition events. The bold values indicate the baseline operating point used in this study, which are the starting points for the investigated parameter sweeps.

At various combinations of operating conditions, the glow-plug temperature is the primary variable that has been varied for influencing the PI tendency. Similar to other studies [35], the spark timing was deliberately set to a late timing to distinguish PI cycles from regular combustion cycles during post-processing and provide sufficient time for the PI to occur. Spark timing was kept close to TDC to allow to distinguish PI cycles from regular cycles as well as provide the whole compression phase for the PI to happen. This results in a center of combustion (CA50) to be around 30 °CAaTDC for methanol and 8 °CAaTDC for hydrogen. This approach identifies PI cycles based on the heat release rate (HRR) with a threshold of 5 J/°CA because this value looks reasonable in terms of a stable evaluation of the combustion considering the noise on the raw pressure signal. In initial post-processing attempts, the crank angle at which 5% of the fuel has been burned (CA05) was used for PI identification, as it is a common method for analyzing engine burn delay. However, since hydrogen showed to ignite also very early in the compression stroke while methanol ignition occurs towards TDC, the CA05 value is strongly influenced by the assumption on the wall heat transfer model (Woschni) used in post-processing of the HRR [36,37]. Therefore, a threshold on the HRR of 5 J/°CA has been preferred to the CA05 as a metric to identify more precisely the start of the heat release. Moreover, CA05 already includes also the initial phases of turbulent flame propagation, which can also be dependent on the operating conditions. If the 5 J/°CA HRR threshold is reached before the spark, the cycle is classified as a PI cycle, as the ignition of the mixture is initiated by the glow-plug. Interestingly, there is a transition phase, in which a combination of PI and standard ignition occurs. Two flame fronts are initiated by both the spark-plug and the glow-plug, which can be observed as two distinct peaks in the heat release rate (HRR): one occurring significantly before the spark timing, and the other shortly after. This phenomenon will be investigated further in future studies using OH^* chemiluminescence via an optical access to the engine.

A PID controller actively regulates the glow-plug power to ensure stable glow-plug temperatures. The controller is necessary because combustion affects the glow-plug temperature: early start of combustion caused by an increase in glow-plug temperature results in higher combustion temperatures. This tends to increase the glow-plug temperature further. To keep the glow-plug to a desired temperature, this must be counteracted by reducing glow-plug power. A solid-state relay regulates this power, controlled precisely by the engine control unit via a pulse width modulation (PWM) signal. This setup allows stable glow-plug temperature control within ±5 K.

To accurately determine the glow-plug temperature at which PI occurs, the setpoint temperature of the glow-plug is incrementally increased in steps of 10 K. To gain further insight into the transition mechanism, in-cylinder pressure traces for multiple cycles are shown in Fig. 2, which explains the evaluation methods used in this study. Different PI ratios, defined as the fraction of pre-ignition cycles occurring at a given operating condition, are illustrated using representative cycles close to the average cycle and two cycles representing the standard deviation. The standard deviation of $\sigma = 1$ has been used for representation purposes to give an estimation of the cycle-to-cycle variation. The focus is to show the shift in ignition time for the different glow-plug temperatures.

The average PI cycle shifts gradually toward earlier ignition timing before the spark event for methanol. In contrast, hydrogen exhibits a distinctly different behavior: once PI occurs in 10% of the cycles, ignition timing immediately advances to approximately −60 °CAaTDC. Notably, cycles within the intermediate range of −40 °CAaTDC to −15 °CAaTDC are not observed, highlighting the abrupt nature of this transition. A noteworthy observation is that the pressure rise rate associated with very early hydrogen injection timings is lower compared to later injection timings. This phenomenon can be attributed to the exceptionally low pressure conditions present during early injection, which are not representative of typical engine operation, as ignition is generally initiated near TDC.

3.2. Numerical

Two different numerical tools are used in this work to analyze and interpret the experimental data. First, numerical simulations are used to analyze ignition delay times. The ITV in-house code *FlameMaster* has been utilized for this purpose. A skeletal reaction mechanism developed in [29] was used for methanol, while the NUIG 1.3 mechanism [38] was adopted for hydrogen. A simplified 0D setup with constant volume assumption has been employed to determine ignition delay times as a function of temperature, pressure, and air–fuel ratio, which are key parameters analyzed in this study.

Second, suggested in the literature, the mixture composition near hot spots significantly influences hot-surface ignition. This aspect has been investigated with 3D RANS simulations performed with CONVERGE CFD v3.1. For this scope, a previously validated simulation

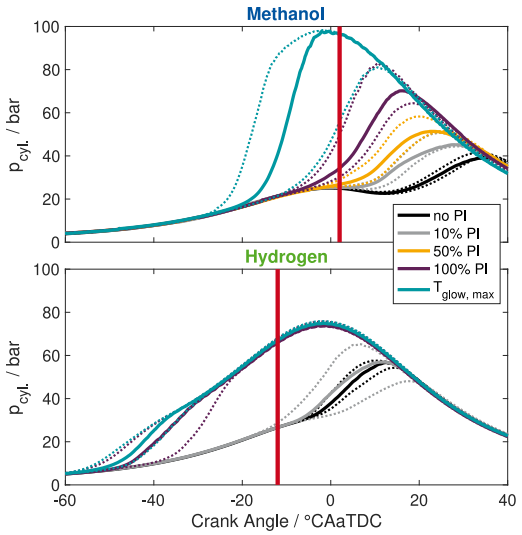


Fig. 2. Pressure traces at a constant operation point for methanol and hydrogen with various glow-plug temperatures leading to different PI ratios. Solid lines represent a cycle close to the average cycle, while dashed lines indicate the standard deviation of $\sigma = 1$ as a common value for rating combustion stability in engines. The red line is the ignition timing. The data was recorded at the baseline conditions. Vertical red lines represent the set spark timing for the different cases. (For interpretation of the references to color in this figure legend, the reader is referred to the web version of this article.)

setup [29,30,33] has been used to numerically investigate mixture formation and temperatures around the glow-plug to support the discussion of the experimental findings. The mesh and model settings have been applied as described in [30], with modifications only to the piston geometry to match the increased compression ratio of the experimental setup. A glow-plug has been included in the model as shown in Fig. 1b featuring a refined mesh size of 0.25 mm around the glow-plug to resolve the thermal boundary layer better.

In this study, only non-reactive simulations have been performed as they are sufficient to determine the mixture and unburned temperature. The injector pipe geometry has been incorporated into the model for gaseous hydrogen injection. The pipe tips have been defined as *inflow boundary condition*, ensuring an accurate representation of hydrogen injection dynamics based on the injector parameters, including opening and closing timings.

4. Results and discussion

The proposed methodology has been applied to various parameter variations, analyzing the effect of different boundary conditions on PI. For example, Fig. 3 illustrates the variation in end compression pressure (ECP). The plot presents the ignition timing of the fuel relative to the spark timing (dashed line) for three different ECP values, considering different glow-plug temperatures.

In the case of methanol, a clear gradual increase to 100% PI is observed. In contrast, for hydrogen, once PI are detected in 10% of the cycles, the ignition timing shifts abruptly toward earlier values. Consequently, the 10% threshold was chosen to define the temperature at which PI occurs. Also, it is used in the following to compare PI tendencies of hydrogen to methanol.

The plots highlight a fundamental difference between the two fuels. It is well established in knock and auto-ignition studies that higher pressures generally reduce ignition delay times for fuels. This trend is evident in the experiments with methanol, where increasing the pressure from 20 bar to 30 bar reduces the glow-plug temperature required for reaching 10% PI threshold from 1053 K to 1013 K. Therefore, it can be suggested that higher loads and pressures are likely to enhance the engine's tendency to cause PI. In contrast, hydrogen exhibits an opposite trend, requiring an increase in glow-plug temperature from 1023 K to 1093 K as the pressure rises from 25 bar to 35 bar. This suggests that hydrogen PI is less likely to occur at higher loads with increased pressure. Moreover, the glow-plug temperature required for hydrogen PI is approximately 30 K higher than that of methanol, although methanol benefits from cooling effects due to fuel vaporization from liquid direct injection. This will be explained in more detail below.

As an overview, Fig. 4 summarizes the effect of surface temperature on the onset of 10% PI for all parameters investigated. Generally, methanol requires a lower hot-spot temperature for PI compared to hydrogen. In particular, hydrogen requires a temperature of around 1100 K, which aligns with previous experimental studies [4]. The uncertainty bars in Fig. 4 account for two primary sources of uncertainty: the thermocouple accuracy of ±1.5 K and the temperature binning size of 10 K.

In terms of the effect of engine speed on PI, both fuels exhibit similar behavior. Increasing engine speed raises the required glow-plug temperature to initiate PI. This can be attributed to the shorter auto-ignition time, as the time scale decreases with increasing engine speed.

Injection timing has an impact on PI events for both fuels. In the case of methanol, the glow-plug temperature is higher for both early and late injection timings. In contrast, the highest temperature for hydrogen is observed at the later timing of −260 °CAaTDC. The different behavior is mainly due to differences in the injector types and fuel mixing. Fig. 5 shows the equivalence ratio and temperature in the glow-plug area for both fuels. For hydrogen with PFI, early injection timing leads to the air-hydrogen mixture being directed toward the glow-plug. This results early in the compression stroke to a locally rich mixture near the glow-plug and significantly influences PI by giving the mixture more time for ignition. Later injection timings up to −260 °CAaTDC lead to a later and slower increase of the equivalence ratio. This leads to reduced time for the mixture's ignition. Injection of hydrogen at −240 °CAaTDC causes a significantly earlier peak of the equivalence ratio because the intake valve is already closing when fuel is injected into the intake manifold. The temperature is similar for all cases except for −320 °CAaTDC as cold hydrogen is led directly toward the glow-plug. In DI with methanol, there are two competing effects influencing the auto-ignition behavior around the glow-plug: local cooling due to fuel evaporation and local air–fuel ratio. CFD results show that early injections result in more fuel being directed toward the cylinder-head and glow-plug as in the hydrogen case. However, since methanol has a very high heat of vaporization, the fuel evaporation results in a locally lower temperature of the mixture around the glow-plug during the compression stroke as visible in Fig. 5. For later injection timings, the fuel evaporates on the surface of the piston as the piston is closer to the cylinder-head. Moreover, later timings result in leaner mixtures near the glow-plug which would increase the required glow-plug temperature. However, the cooling due to the vaporization of methanol is the dominant effect in this trade-off. Indeed, the observed PI trends are correlated with the observed local temperature trends around the glow-plug during compression. Given the strong influence of mixture formation on PI trends, these effects can be utilized in engine calibration and design. In PFI operation with hydrogen, the geometry of the intake ports and valves can be optimized to direct the mixture away from hot surfaces. In DI mode with methanol, the injector and nozzle design directly influence PI tendencies. For liquid fuels, injecting toward potential hot spots can enhance cooling, whereas for hydrogen DI, avoiding injection into hot spots during the early stages can mitigate PI.

Valve timing does not significantly affect methanol DI operation, as it primarily influences airflow, which has a minor impact on hot surface temperatures and local air–fuel mixing. However, for hydrogen PFI

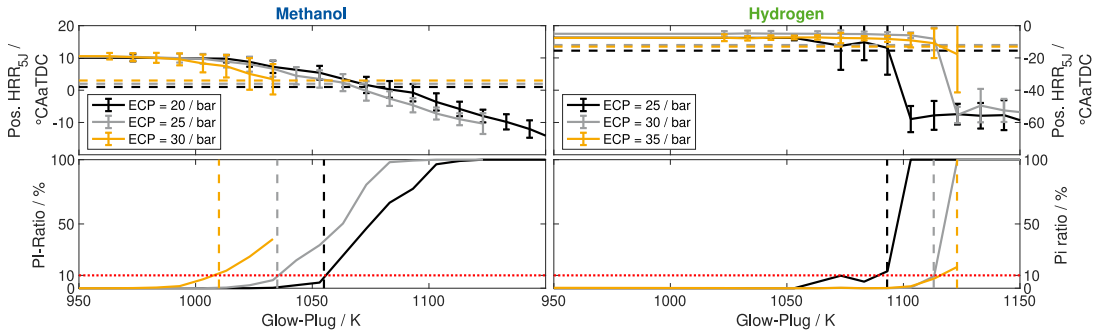


Fig. 3. Filtered PI cycles at different glow-plug temperatures and varying ECP for methanol (left) and hydrogen (right). The upper row represents the first occurrence of 5 J/°CA with error bars indicating the standard deviation in the detected cycles at the set glow-plug temperature. The lower row shows the pre-ignition ratio (0%–100%). Vertical dashed lines represent the glow-plug temperature at which 10% of the cycles are ignited by the glow-plug.

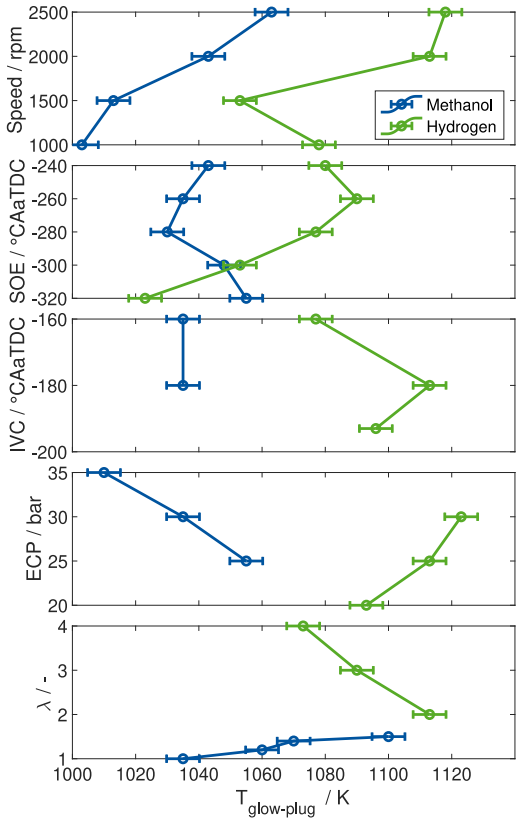


Fig. 4. Required glow-plug temperature resulting in a 10% pre-ignition (PI) ratio for methanol and hydrogen for all the investigated parameters. The error bars represent the measurement uncertainties due to binning and the thermocouple.

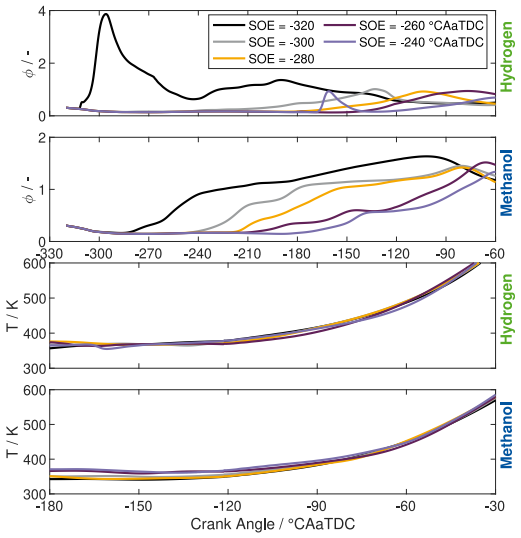


Fig. 5. Equivalence ratio and temperature near the glow-plug according to non-reactive CONVERGE RANS CFD engine simulations for both fuels at all SOE timings.

operation, valve timing strongly affects hydrogen flow around the glow-plug. If the intake valve closes at bottom dead center (−180 °CAaTDC), there is no mixture backflow into the intake ports. Closing the intake valve at −160 °CAaTDC results in a backflow of the mixture into the intake ports, allowing hydrogen to flow past the glow-plug as it is located between the intake valves as shown in Fig. 1b. When the intake valve closes at −193 °CAaTDC, residual hydrogen from the previous cycle remains near the intake valve and is immediately drawn into the cylinder when the valve reopens, directing it toward the glow-plug in the next cycle. This will provide the mixture more time to ignite.

Next, the air–fuel ratio (λ) and end-compression pressure (ECP) are analyzed in parallel, as both parameters strongly impact thermodynamic conditions important for homogeneous ignition delay times. For methanol, the observed trends align with expectations: increasing λ raises the required glow-plug temperature for pre-ignition (PI) while increasing ECP lowers it. These trends are well predicted by 0D ignition delay time simulations (Fig. 6). The plot in Fig. 6 illustrates ignition delay times for both fuels as a function of pressure and temperature. Methanol exhibits a monotonic trend concerning pressure and air–fuel ratio, where higher pressures consistently reduce ignition delay times while an increase in λ increases it. Therefore, the observed trends can be reasonably explained with the according reaction kinetics.

In contrast, hydrogen shows mainly inverted trends with glow-plug temperature in comparison to methanol. The analysis of ignition delay times explains this behavior. Hydrogen PI typically occurs early in the compression stroke, at pressures ranging from 2 bar to 10 bar and temperatures between 1070 K and 1130 K. Within this operating range, hydrogen ignition delay times are highly non-linear. The ignition delay time is plotted against pressure for the selected temperature range to clarify this effect. This reveals a pronounced increase in ignition delay time (by up to a factor of 100) as pressure rises during compression. Increasing ECP requires higher intake pressures, causing higher pressures earlier in the compression stroke, which suppresses PI. This explains why hydrogen either causes PI early in the compression stroke or results in normal combustion. If PI is not triggered during compression, the rising pressure further increases ignition delay time, strongly differentiating hydrogen from methanol. This also explains the

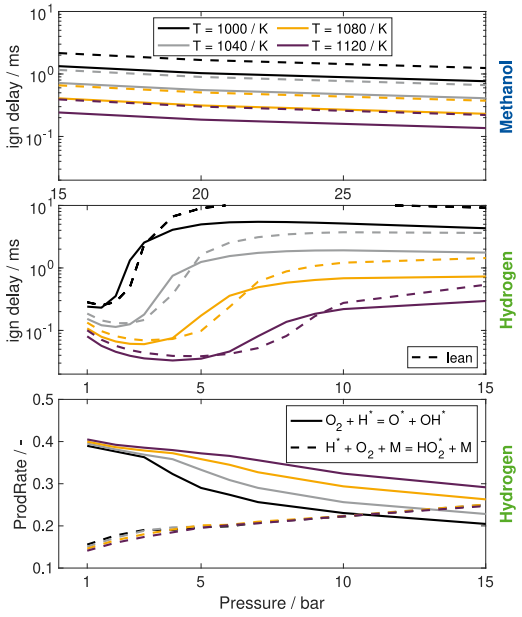


Fig. 6. Numerically simulated 0D ignition delay times for methanol (solid $\lambda = 1$ and dashed $\lambda = 1.6$ [lean]) and hydrogen (solid $\lambda = 2.0$ and dashed $\lambda = 4.0$ [lean]) at various temperature and pressure conditions. The x- and y-axis represent the ranges where PI at the specific fuel is typically observed.

SOE trends. As the fuel–air mixture reaches the glow-plug early at low pressures, ignition delay is significantly reduced, and the time provided to ignite is enhanced.

To elucidate the observed behavior of hydrogen, a reaction flux analysis was conducted for the hydrogen cases. The first relevant pathway is the chain-branching reaction,

$$O_2 + H^* \longrightarrow O^* + OH^*,$$

which exhibits a strong temperature dependence; higher temperatures accelerate this step. In contrast, the second pathway,

$$H^* + O_2 + M \longrightarrow HO_2{}^* + M,$$

acts as a chain-terminating reaction. The flux analysis reveals that this pathway is only weakly temperature-dependent at low pressures, but its contribution increases markedly with pressure. At elevated pressures, its temperature dependence within the investigated operating range becomes negligible. Overall, the results demonstrate that increasing pressure promotes chain termination, thereby reducing the overall reaction rate and leading to longer ignition delay times.

Finally, the 0D simulations also explain the λ trend. Increasing λ results in an increase in ignition delay time towards higher pressures. Consequently, the ignition delay time remains lower throughout the compression stroke at leaner mixtures, requiring lower glow-plug temperatures to obtain PI. Building upon these findings, several strategies can be considered to mitigate pre-ignition (PI) in hydrogen engine applications. One promising approach is the use of direct hydrogen injection (DI) with later injection timings. This technique reduces the residence time of the fuel–air mixture near potential hot spots and takes advantage of the naturally increased ignition delay at higher pressures. Furthermore, late injection helps maintain a richer mixture during the compression, which can further prolong the ignition delay due to the earlier increase of ignition delay times with increasing pressure according to Fig. 6. However, it should be noted that implementing later injection timings may require higher injection pressures and could result in increased nitrogen oxide (NO_x) formation due to mixture inhomogeneities. In addition to optimizing injection timing, modifying the mixing process and charge motion within the cylinder can help optimize the hydrogen distribution away from hot surfaces; this can be achieved through adjustments to intake port design or injector geometry. Finally, employing optical spark plugs allows for precise detection of PI locations after prototype engine assembly. Based on these observations, subsequent modifications to injector position or piston design can be made to further reduce the risk of pre-ignition.

5. Conclusion

This study analyzed the hot-spot-induced pre-ignition (PI) tendencies of methanol and hydrogen with the assistance of an instrumented glow-plug with a focus on key parameters such as glow-plug temperature, injection timing, air–fuel ratio (λ), end-compression pressure (ECP), and engine speed. The results demonstrate that methanol and hydrogen exhibit distinct PI behaviors influenced by mixture formation, reaction kinetics, and pressure-dependent ignition delay.

For methanol, PI events occur progressively as glow-plug temperature increases, with a smooth transition from standard ignition to complete PI cycles. In contrast, hydrogen has been observed to abruptly shift to 100% PI once a critical glow-plug temperature is exceeded. This difference arises from hydrogen's strong pressure dependence on ignition delay, causing either early PI during compression or normal spark-ignited combustion with no intermediate transition for the tested conditions.

Injection timing significantly impacts PI behavior. In DI methanol combustion, early injection leads to fuel redirection and local cooling near the glow-plug, reducing PI risk. In PFI hydrogen operation, early injection increases PI risk due to mixture accumulation near the glow-plug, while later injection reduces it. This highlights the importance of optimizing injector placement and timing to mitigate hot-spot-induced PI.

End compression pressure (ECP) and λ influence PI differently for each fuel. For methanol, higher ECP lowers the required glow-plug temperature for PI due to reduced ignition delay, while leaner mixtures increase it. In contrast, hydrogen shows the opposite behavior.

Overall, these findings provide valuable insights into hot-spot-induced PI mechanisms and mitigation strategies. Optimizing injection timing, leveraging pressure-dependent ignition delay effects, and operating at higher engine speeds can help control PI in both methanol and hydrogen combustion systems. These results are critical for improving engine efficiency and reliability, particularly in advanced combustion concepts utilizing alternative fuels. In compression ignition (CI) engines, a temperature-controlled hot-spot-induced ignition (e.g., with a glow-plug) appears to be a viable combustion concept in combination with methanol. In contrast, for hydrogen, hot-spot-induced ignition in engines should be avoided. Because of the inverse pressure dependence of the ignition delay time, PI occurs more likely early in the compression stroke, while it will be suppressed at higher pressures towards top dead center. Hence, controlling ignition in hydrogen CI engines by hot surfaces seems infeasible. Finally, this study provides a unique dataset for further experimental and numerical investigation of hot-spot-induced ignition.

Novelty and significance statement

The novelty of this research lies in its investigation of hot-spot surface ignition within a spark-ignition single-cylinder engine fueled by methanol and hydrogen. The hot-spot has been artificially generated with a prototype glow-plug that features an integrated thermocouple to measure the hot-spot temperature. The test matrix consisted of a cycle-resolved parametric study over injection timing, equivalence ratio, end-of-compression pressure, and engine speed in which 1000 cycles per condition are recorded for statistical relevance. To further analyze the results, 0D ignition-delay and 3D RANS CFD simulations support the observed experimental trends. This work provides the first direct comparison of methanol and hydrogen ignition behavior and offers

hot-spot temperature measurements. Moreover, the generated dataset is unique in its kind since similar measurements with these fuels featuring a hot-spot have not been found in literature. These results provide insights to develop strategies to prevent abnormal combustion and to optimize glow-plug-assisted compression ignition concepts.

CRediT authorship contribution statement

D. Golc: Conceptualization, Methodology, Investigation, Formal analysis, Visualization, Writing – original draft. **S. Esposito:** Conceptualization, Methodology, Writing – original draft, Writing – review & editing. **M. Khosravi:** Conceptualization, Resources, Writing – review & editing. **J. Beeckmann:** Funding acquisition, Project administration, Supervision, Writing – review & editing. **H. Pitsch:** Funding acquisition, Project administration, Supervision, Writing – review & editing.

Declaration of competing interest

The authors declare that they have no known competing financial interests or personal relationships that could have appeared to influence the work reported in this paper.

Acknowledgments

The authors gratefully acknowledge the received funding from the European Research Council (ERC) under the European Union's Horizon 2020 research and innovation program (Grant agreement No. 101054894) and the computing time provided at the NHR Center NHR4CES at RWTH Aachen University (project number p0020900). Thanks also to the Research Unit FOR2401, funded by the German Research Foundation (DFG) and Convergent Science for providing CONVERGE licenses and tech. support.

References

[1] H. Pitsch, The transition to sustainable combustion: Hydrogen- and carbon-based future fuels and methods for dealing with their challenges, Proc. Combust. Inst. 40 (1) (2024).
[2] S. Sollai, A. Porcu, V. Tola, F. Ferrara, A. Pettinau, Renewable methanol production from green hydrogen and captured CO2: A techno-economic assessment, J. CO2 Util. 68 (2023).
[3] Y.-H. Pu, Q. Dejaegere, M. Svensson, S. Verhelst, Renewable methanol as a fuel for heavy-duty engines: A review of technologies enabling single-fuel solutions, Energies 17 (7) (2024).
[4] R. Rajasegar, A. Srna, I. Barbery, R. Novella, On the phenomenology of hot-spot induced pre-ignition in a direct-injection hydrogen-fueled, heavy-duty, optical-engine, in: 2023 JSAE/SAE Powertrains, Energy and Lubricants International Meeting, 2023.
[5] F. Fruzza, H. Chu, R. Lamioni, T. Grenga, C. Galletti, H. Pitsch, The importance of Soret effect, preferential diffusion, and conjugate heat transfer for flashback limits of hydrogen-fueled perforated burners, Proc. Combust. Inst. 40 (1) (2024).
[6] X. Liu, J. Sim, V. Raman, Y. Viollet, A.S. AlRamadan, E. Cenker, H.G. Im, Computational investigation of a methanol compression ignition engine assisted by a glow plug, Int. J. Engine Res. (2024).
[7] S. Verhelst, J.W.G. Turner, Hydrogen-fueled spark ignition engines, in: E.-A. Tingas (Ed.), Hydrogen for Future Thermal Engines, Springer International Publishing, 2023, pp. 329–351.
[8] W.L. Mitchell, T.A. Litzinger, D.A. Santavicca, Neat methanol combustion in a D.I. Diesel engine using catalytically coated glow plugs, in: International Fuels & Lubricants Meeting & Exposition, 1991.
[9] W.H. Haight, P.C. Malte, Methanol preignition temperature behavior, in: International Fuels & Lubricants Meeting & Exposition, 1991.
[10] W.A. Goetz, C.G. Barringer, M.A. Bozzelli, Utilizing neat methanol and glow plug ignition in DI diesels: Laboratory testing of a single and multi-cylinder engine, in: International Congress & Exposition, 1994.
[11] C.J. Mueller, M.P. Musculus, Glow plug assisted ignition and combustion of methanol in an optical DI diesel engine, in: International Spring Fuels & Lubricants Meeting, 2001.
[12] R.A. Krishnan, K. Panda, A. Ramesh, Simulation studies on glow plug assisted neat methanol combustion in a diesel engine, in: WCX SAE World Congress Experience, 2022.
[13] P. Rameez, M. Mohamed Ibrahim, A comprehensive review on the utilization of hydrogen in low temperature combustion strategies: Combustion, performance and emission attributes, J. Energy Inst. 113 (2024).
[14] Z. Li, C. Zhai, X. Zeng, K. Shi, X. Wu, T. Ma, Y. Qi, Review of pre-ignition research in methanol engines, Energies 18 (1) (2024) 133.
[15] J. Mutzke, R. Stone, J. Williams, Surface pre-ignition measurements of fuel components and their mixtures, Fuel 233 (2018) 513–518.
[16] H. Goyal, P. Jones, A. Bajwa, D. Parsons, S. Akehurst, M.H. Davy, F.C. Leach, S. Esposito, Design trends and challenges in hydrogen direct injection (H2DI) internal combustion engines – A review, Int. J. Hydrog. Energy 86 (2024) 1179–1194.
[17] S. Verhelst, T. Wallner, Hydrogen-fueled internal combustion engines, Prog. Energy Combust. Sci. 35 (6) (2009) 490–527.
[18] C. Chi, A. Abdelsamie, D. Thévenin, Direct numerical simulations of hotspot-induced ignition in homogeneous hydrogen-air pre-mixtures and ignition spot tracking, Flow Turbul. Combust. 101 (1) (2018) 103–121.
[19] J. Melguizo-Gavilanes, L. Boeck, R. Mével, J. Shepherd, Hot surface ignition of stoichiometric hydrogen-air mixtures, Int. J. Hydrog. Energy 42 (11) (2017) 7393–7403.
[20] H. Chu, T. Li, H. Bai, Z. Li, H. Pitsch, Numerical investigation of hot-surface ignition of hydrogen-air mixtures, 2025.
[21] T. Howarth, E. Hunt, A. Aspden, Thermodiffusively-unstable lean premixed hydrogen flames: Phenomenology, empirical modelling, and thermal leading points, Combust. Flame 253 (2023).
[22] S. Shashidharan, R.K. Velamati, S. Kumar, J. Edacheri Veetil, Hot surface ignition of H2-air and CH4– H2-air mixtures for various equivalence ratios and heating rates, Int. J. Hydrog. Energy 53 (2024) 770–779.
[23] H. Chu, T. Li, H. Bai, Z. Li, H. Pitsch, Numerical investigation of hot-spot surface ignition of hydrogen-air mixtures, in: Proceedings of the 12th European Combustion Meeting, Edinburgh, Scotland, UK, 2025.
[24] Z. Yang, D. Li, L. Wang, Research on the hot surface ignition of hydrogen-air mixture under different influencing factors, Int. J. Energy Res. 42 (12) (2018) 3966–3976.
[25] S. Guo, J. Liu, C. Zhao, L. Wang, Z. Yang, Research on pre-ignition in hydrogen internal combustion engines based on characteristic parameters of hot spot, Int. J. Hydrog. Energy 65 (2024) 548–554.
[26] L. Boeck, J. Melguizo-Gavilanes, J. Shepherd, Hot surface ignition dynamics in premixed hydrogen–air near the lean flammability limit, Combust. Flame 210 (2019) 467–478.
[27] R. Mével, J. Melguizo-Gavilanes, L. Boeck, J. Shepherd, Experimental and numerical study of the ignition of hydrogen-air mixtures by a localized stationary hot surface, Int. J. Heat Fluid Flow 76 (2019) 154–169.
[28] R.K. Velamati, S. Raj, P. Parthasarathy, J.E. Veetil, Ignition studies of hydrogen-air mixtures over hot wire, Int. J. Hydrog. Energy 48 (4) (2023) 1582–1595.
[29] F. Loffredo, S. Esposito, M. Buenaflor, D. Golc, S. Girhe, J. Beeckmann, H. Pitsch, Skeletal mechanism for methanol oxidation and nitrogen oxides predictions: Application to Spark-Ignition (SI) engines, in: European Combustion Meeting 2023, 2023.
[30] S. Esposito, A. Chaychizadeh, D. Golc, R. Hesse, J. Beeckmann, H. Pitsch, 3D-CFD RANS methodology to predict engine-out emissions with gasoline-like fuel and methanol for a DISI engine, SAE Int. J. Adv. Curr. Pr. Mobil. 5 (3) (2022) 1364–1376.
[31] E. Malfi, S. Esposito, M. De Felice, H. Pitsch, S. Pischinger, V. De Bellis, Phenomenological model for unburned hydrocarbon emissions from spark-ignition, pre-chamber, and dual-fuel internal combustion engines, Int. J. Engine Res. (2024).
[32] R. Hesse, C. Schwenzer, R. Glaznev, S. Esposito, Y. Fenard, H. Pitsch, J. Beeckmann, Experimental-based laminar flame speed approximation formulas of efficiency-optimized biofuels for SI-engine modeling, SAE Int. J. Adv. Curr. Pr. Mobil. 5 (3) (2022) 1344–1353.
[33] S. Esposito, E. Malfi, M. De Felice, D. Golc, J. Beeckmann, H. Pitsch, V. De Bellis, Methanol fuelling of a spark-ignition engine: experiments and 0D/1D predictive modelling for combustion, performance, and emissions, Fuel 393 (2025).
[34] O. Budak, F. Hoppe, B. Heuser, S. Pischinger, U. Burke, A. Heufer, Hot surface pre-ignition in direct-injection spark-ignition engines: Investigations with tailor-made fuels from biomass, Int. J. Engine Res. 19 (1) (2018) 45–54.
[35] S. Pischinger, M. Günther, O. Budak, Abnormal combustion phenomena with different fuels in a spark ignition engine with direct fuel injection, Combust. Flame 175 (2017) 123–137.
[36] J. Krishnanunni, D. Bhatia, L.M. Das, Experimental and modelling investigations on the performance and emission characteristics of a single cylinder hydrogen engine, Int. J. Hydrog. Energy 42 (49) (2017-12) 29574–29584.
[37] X. Dou, M. Yosri, M. Talei, Y. Yang, Impact of wall heat transfer modelling in large-eddy simulation of hydrogen knocking combustion, Int. J. Hydrog. Energy 62 (2024-04) 405–417.
[38] S. Panigrahy, A.A.E.-S. Mohamed, P. Wang, G. Bourque, H.J. Curran, When hydrogen is slower than methane to ignite, Proc. Combust. Inst. 39 (1) (2023) 253–263.